



# Hydrogen solubility and permeability of Nb–W–Mo alloy membrane

Y. Awakura<sup>a</sup>, T. Nambu<sup>b</sup>, Y. Matsumoto<sup>c</sup>, H. Yukawa<sup>a,\*</sup>

<sup>a</sup> Department of Materials Science and Engineering, Graduate School of Engineering, Nagoya University, Furo-cho, Chikusa-ku, Nagoya, Aichi 464-8603, Japan

<sup>b</sup> Department of Materials Science and Engineering, Suzuka National College of Technology, Shiroko-cho, Suzuka, Mie 510-0294, Japan

<sup>c</sup> Department of Mechanical Engineering, Oita National College of Technology, Maki, Oita 870-0152, Japan

## ARTICLE INFO

### Article history:

Received 2 July 2010

Received in revised form 16 October 2010

Accepted 22 October 2010

Available online 4 November 2010

### Keywords:

Hydrogen permeable membrane

Nb-based alloy

Hydrogen solubility

Resistance to hydrogen embrittlement

Hydrogen permeability

## ABSTRACT

The alloying effects of molybdenum on the hydrogen solubility, the resistance to hydrogen embrittlement and the hydrogen permeability are investigated for Nb–W–Mo system. It is found that the hydrogen solubility decreases by the addition of molybdenum into Nb–W alloy. As a result, the resistance to hydrogen embrittlement improves by reducing the hydrogen concentration in the alloy. It is demonstrated that Nb–5 mol%W–5 mol%Mo alloy possesses excellent hydrogen permeability without showing any hydrogen embrittlement when used under appropriate hydrogen permeation conditions, i.e., temperature and hydrogen pressures.

© 2010 Elsevier B.V. All rights reserved.

## 1. Introduction

Palladium (Pd) and its alloys are well-known as hydrogen permeable materials to be used for the separation and purification of high purity hydrogen gas [1]. Recently, there has been a great demand for the development of new hydrogen permeable alloys to be substituted for currently used Pd-based alloys, in order to reduce material cost as well as to improve the hydrogen permeability [2–5]. Niobium (Nb) is less expensive than palladium and exhibits the highest hydrogen permeability among metals [6], so it is one of the most promising materials for hydrogen permeable membranes. However, there is still a large barrier to the practical use due to its poor resistance to hydrogen embrittlement.

Recently, the mechanical properties of niobium in hydrogen gas atmosphere at high temperature have been investigated by the *in situ* small punch (SP) test method [7,8]. It was found that the ductile-to-brittle transition occurs at the hydrogen concentration around H/M = 0.25 at the temperature range between 573 and 773 K without showing any micro-structural changes (i.e., phase transition or precipitation of secondary phase) [9]. This fact suggests that the resistance to hydrogen embrittlement of niobium will be improved by keeping the hydrogen concentration below this critical value during the practical hydrogen permeation.

On the other hand, the hydrogen diffusion in metal membrane is generally the rate-limiting process of the total reaction of the

hydrogen permeation through it. Therefore, the hydrogen flux,  $J$ , through the membrane with a thickness of  $d$  can be expressed by the following diffusion equation,

$$J = -cB \frac{\Delta\mu}{d}, \quad (1)$$

where  $c$  is the hydrogen concentration,  $B$  is the mobility and  $\Delta\mu$  is the difference of hydrogen chemical potential between the inlet and outlet sides of the membrane. Assuming that the equilibrium conditions are achieved at both inlet and outlet sides of the membrane with the hydrogen pressures of  $P_{\text{inlet}}$  and  $P_{\text{outlet}}$ , the difference of hydrogen chemical potential can be expressed as follows [10].

$$\Delta\mu = \frac{1}{2} RT \ln \left( \frac{P_{\text{inlet}}}{P_{\text{outlet}}} \right), \quad (2)$$

where  $R$  is gas constant and  $T$  is absolute temperature. As expressed in Eq. (1), high hydrogen flux,  $J$ , will be expected when the parameter  $c \times \Delta\mu$  is large for the designed alloy membrane at a given hydrogen permeation conditions, i.e., inlet and outlet hydrogen pressures [10].

From these results, a concept for alloy design of Nb-based hydrogen permeable membrane has been proposed [10,11]. Following this concept, Nb–5 mol%W alloy with a single solid solution phase have been designed and developed which possesses high hydrogen permeability without showing any hydrogen embrittlement when used under appropriate permeation conditions [10].

In this study, the concept has been applied to Nb–W–Mo ternary system in order to improve further the resistance to hydrogen

\* Corresponding author.

E-mail address: [hiroshi@numse.nagoya-u.ac.jp](mailto:hiroshi@numse.nagoya-u.ac.jp) (H. Yukawa).

**Table 1**  
Nominal compositions of the samples.

Sample	Concentration, $c$ /(mol%)		
	W	Mo	Nb
Nb–5W	5	–	bal.
Nb–5W–5Mo	5	5	bal.
Nb–5W–10Mo	5	10	bal.
Nb–5W–15Mo	5	15	bal.

embrittlement at high hydrogen pressures as well as the hydrogen permeability of Nb–W alloy. The alloying effects of molybdenum into Nb–W alloy on the hydrogen solubility, the resistance to hydrogen embrittlement and the hydrogen permeability are investigated in a fundamental manner.

## 2. Experimental procedure

### 2.1. Sample preparation

The purities of the raw materials used in this study are 99.96 mass% for niobium and 99.95 mass% for tungsten and molybdenum. Nb–W–Mo alloys are prepared by using tri-arc furnace in a purified argon gas atmosphere. The nominal compositions of the alloys prepared in this study are listed in Table 1. According to the Nb–W, Nb–Mo and Mo–W equilibrium phase diagrams, all the alloys are composed of a single solid solution phase with simple bcc crystal structure [12].

### 2.2. Hydrogen pressure-composition-isotherm (PCT) measurement

In order to examine the hydrogen solubility for Nb–5 mol%W– $x$  mol%Mo ( $x = 5, 10, 15$ ) alloys, the pressure-composition-isotherms (PCT) are measured by using a Sieverts-type apparatus. A small piece of the sample is placed in a cell and then the cell is evacuated by using TMP pump. Subsequently, it is heated up to 773 K, and then high purity hydrogen (99.99999% purity) of about 5 MPa is introduced and cooled down to room temperature. This process is repeated at least three times prior to the PCT measurement in order to activate the sample surface for the hydrogen absorption and desorption reactions to take place smoothly. The PCT curves are measured at 673–773 K and up to about 5 MPa of hydrogen pressure.

### 2.3. In situ small punch (SP) test

The mechanical properties of Nb–5 mol%W–5 mol%Mo alloys in hydrogen gas atmosphere are investigated quantitatively by the *in situ* small punch (SP) test method. Plate-shaped specimens of about 10 mm  $\times$  10 mm with a thickness of about 0.6 mm are prepared by using a wire-electric discharge machine. Both sides of the specimens are mechanically polished by using alumina abrasive paper followed by the final polishing. The thickness of the specimen is reduced to  $0.5 \pm 0.01$  mm by the final polishing with 0.3  $\mu$ m  $\text{Al}_2\text{O}_3$  powders. Subsequently, pure palladium of about 200 nm in thickness is deposited at 573 K on both sides of the sample surfaces by using an RF magnetron sputtering apparatus in order to protect the sample surface from oxidation. The Pd-coating on the surface also acts as a catalyst to eliminate the hindrance to the hydrogen dissociation and dissolution reactions on the surfaces of the membrane.

The load-deflection curves are obtained by the *in situ* SP tests conducted under a constant hydrogen pressure of 0.01 MPa at 673 K or 773 K. The plate-shaped specimen is placed in the apparatus and, then punched by a  $\text{Si}_3\text{N}_4$  ball ( $\phi$  2.4 mm in diameter) with a constant loading rate (i.e., the cross-head speed),  $v = 8.3 \times 10^{-3}$  mm/s. The SP absorption energy,  $E_{\text{SP}}$ , is estimated by taking the area under each load-deflection curve until the specimen fails. The detailed explanation of the *in situ* SP test is given elsewhere [7].

### 2.4. Hydrogen permeation test

The hydrogen permeation tests are performed for Nb–5 mol%W–5 mol%Mo alloy at 773 K. Disk specimens of about  $\phi$  12 mm in diameter with a thickness of about 0.5 mm are prepared. They are polished mechanically and coated with pure palladium by the same procedure as mentioned above. For comparison, samples of Nb–5 mol%W and Pd–26 mol%Ag alloys are also prepared.

The disk sample is set into the hydrogen permeation apparatus and then evacuated. Subsequently, it is heated up to 773 K, and then a high purity hydrogen gas (99.99999% purity) is introduced into both sides of the specimen. The inlet and outlet hydrogen pressures applied in this study are listed in Table 2. These hydrogen pressures are determined from the PCT curves so that the hydrogen concentration does not exceed the critical value  $H/M < 0.25$  [7] to avoid the brittle cracking due to hydrogen embrittlement. The hydrogen fluxes,  $J$ , permeated through the disk samples are measured by a conventional gas permeation method. A detailed explanation of the hydrogen permeation test is given elsewhere [13].

**Table 2**  
Pressure conditions of the hydrogen permeation test.

Sample	Hydrogen pressure, $P$ /MPa	
	Inlet	Outlet
Nb–5W–5Mo	0.10	0.01
	0.07	bal.
	0.05	bal.
Nb–5W	0.05	0.01
Pd–26Ag	0.26	0.06

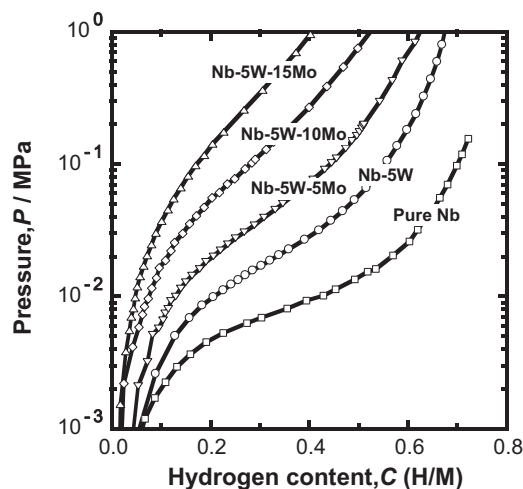


**Fig. 1.** PCT curves for Nb–5 mol%W– $x$  mol%Mo ( $x = 5, 10$  and  $15$ ) alloys measured at 673 K. The PCT curves for pure niobium measured at 673 K [14] and Nb–5 mol%W alloy measured at 673 K [11] are also drawn in the figure.

## 3. Results and discussion

### 3.1. Alloying effects of Mo on the hydrogen solubility of Nb–W alloy

The PCT curves for Nb–5 mol%W– $x$  mol%Mo ( $x = 5, 10, 15$ ) measured at 673 K and 773 K are shown in Figs. 1 and 2, respectively. For comparison, the results for pure niobium reported by Veleckis and Edwards [14] and Nb–5 mol%W reported by Yukawa et al. [11] are also drawn in the figures. As is evident from these figures, the PCT

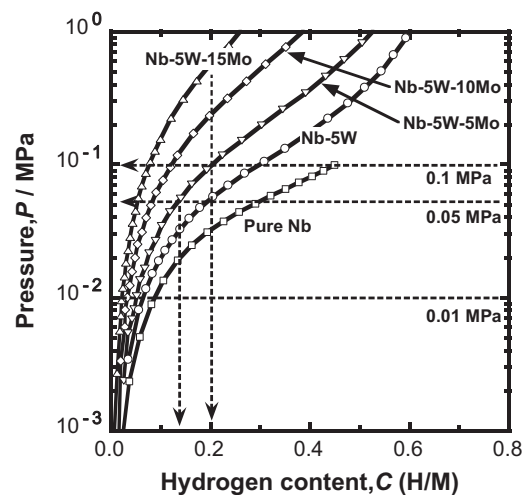


**Fig. 2.** PCT curves for Nb–5 mol%W– $x$  mol%Mo ( $x = 5, 10$ , and  $15$ ) alloys measured at 773 K. The PCT curves for pure niobium measured at 773 K [14] and Nb–5 mol%W alloy measured at 773 K [11] are also drawn in the figure.

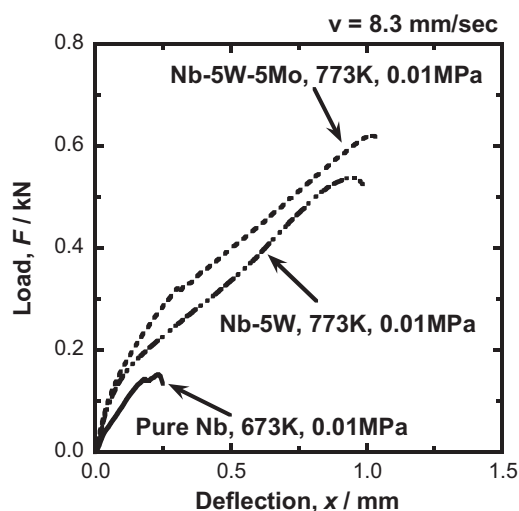


**Fig. 3.** Load–deflection curves for pure niobium measured at 673 K, Nb–5 mol%W and Nb–5 mol%W–5 mol%Mo alloys measured at 773 K at 0.01 MPa of hydrogen pressure.

curve shifts toward the left and upper side with increasing molybdenum content in the alloy, indicating that the amount of dissolved hydrogen in the alloy at a given pressure decreases by the addition of molybdenum. Comparing Fig. 1 with Fig. 2, it is found that the PCT curve also shifts toward left and upper side with increasing temperature.

### 3.2. Mechanical properties of Nb–W–Mo alloy in hydrogen atmosphere

The *in situ* SP tests are conducted at 773 K for Nb–5 mol%W–5 mol%Mo alloy in the hydrogen gas atmosphere of 0.01 MPa. The load–deflection curves are shown in Fig. 3. For comparison, the results of load–deflection curves for pure niobium measured at 673 K and Nb–5 mol%W alloy measured at 773 K at the same pressure condition are also drawn in the figure.

As shown in Fig. 3, the maximum load and deflection for pure niobium measured at 673 K are very small. On the other hand, the load–deflection curve for Nb–5 mol%W–5 mol%Mo alloy measured at 773 K shows very large ultimate load and deflection. Comparing this curve with that for Nb–5 mol%W alloy, it is evident that the ultimate load and deflection increase by the addition of molybdenum into Nb–5 mol%W alloy. This result indicates that the addition of molybdenum gives further solid solution hardening and improves the mechanical properties (i.e., the strength and the ductility) of Nb–5 mol%W alloy in the hydrogen gas atmosphere of 0.01 MPa at high temperature.

The SP absorption energy,  $E_{SP}$ , is estimated from each load–deflection curve shown in Fig. 3 and the results are summarized in Table 3 together with the equilibrium hydrogen concentration at 0.01 MPa estimated from the corresponding PCT curves shown in Figs. 1 and 2.

As shown in Table 3, the SP absorption energy for pure niobium measured at 673 K is very small, indicating that brittle fracture

**Table 3**

SP absorption energies estimated from the load–deflection curves shown in Fig. 3, and the equilibrium hydrogen concentrations at 0.01 MPa of hydrogen pressure.

Sample	Temperature, T/K	SP absorption energy, $E_{SP}$ /J	$c/(H/M)$
Pure Nb	673	0.015	0.42
Nb–5W	773	0.301	0.07
Nb–5W–5Mo	773	0.384	0.05

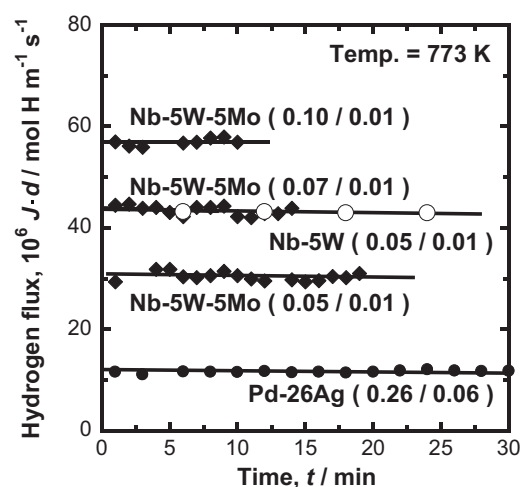


**Fig. 4.** Changes in the normalized hydrogen flux,  $J \cdot d$ , during the measurements at 773 K. The inlet and outlet hydrogen pressures for each measurement are indicated in parentheses in the figure as (inlet/outlet [MPa]).

due to severe hydrogen embrittlement occurs under the hydrogen pressure of 0.01 MPa where a large amount of hydrogen is dissolved in it. On the other hand, the  $E_{SP}$  values for Nb–5 mol%W and Nb–5 mol%W–5 mol%Mo alloys are about 20 and 25 times larger than that value for pure niobium, respectively. The dissolved hydrogen concentrations under 0.01 MPa of hydrogen pressure are about 0.07 and 0.05 (H/M) for Nb–5 mol%W and Nb–5 mol%W–5 mol%Mo alloys, respectively. Thus, the addition of molybdenum into Nb–W alloy or increasing the temperature improves the resistance to hydrogen embrittlement by reducing the hydrogen concentration in the specimen. In fact, Nb–5 mol%W–5 mol%Mo alloy possesses strong resistance to hydrogen embrittlement during hydrogen permeation, as explained later.

### 3.3. Hydrogen permeability

The steady-state hydrogen fluxes,  $J$ , are measured at 773 K for Nb–5 mol%W–5 mol%Mo alloy. It is divided by the inverse of the sample thickness,  $1/d$ , in order to estimate the normalized hydrogen flux,  $J \cdot d$ . It is noted here that atomic hydrogen flux ( $\text{mol H m}^{-1} \text{s}^{-1}$ ) is measured in this study, which is twice as large as gaseous hydrogen flux ( $\text{mol H}_2 \text{m}^{-1} \text{s}^{-1}$ ).

The changes in the normalized hydrogen flux,  $J \cdot d$ , during measurement are shown in Fig. 4. For comparison, the results for Pd–26 mol%Ag and Nb–5 mol%W alloys measured at 773 K are also presented in the figure. The inlet and outlet hydrogen pressures for each measurement are indicated in parentheses in the figure as (inlet/outlet [MPa]).

As shown in Fig. 4, the hydrogen flux is stable and nearly constant during each measurement. The hydrogen flux changes depend on the applied hydrogen pressures. It is found that the hydrogen flux is higher for Nb–5 mol%W alloy than Nb–5 mol%W–5 mol%Mo alloy when the applied pressure condition is the same, (i.e., inlet/outlet = 0.05/0.01 MPa). This fact can be understood in view of the diffusion equation, Eq. (1). The pressure condition is the same so that the difference of hydrogen chemical potential,  $\Delta\mu$ , is the same. However, as shown in Fig. 2, the hydrogen concentration,  $c$ , is higher for Nb–5 mol%W alloy than Nb–5 mol%W–5 mol%Mo alloy at 0.05 MPa of hydrogen pressure. Thus, the parameter  $c \times \Delta\mu$  is larger for Nb–5 mol%W alloy than Nb–5 mol%W–5 mol%Mo alloy in this condition, resulting in the higher hydrogen flux for binary alloy than ternary alloy at the same pressure condition.

On the other hand, the hydrogen flux for Nb–5 mol%W–5 mol%Mo alloy measured under the pressure con-

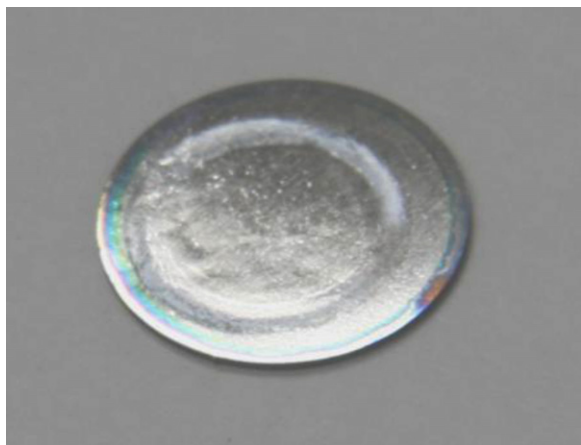


**Fig. 5.** Appearance of the disk sample of Nb–5 mol%W–5 mol%Mo alloy evacuated and cooled down to room temperature after the hydrogen permeation test.

dition of inlet/outlet = 0.1/0.01 MPa is higher than that for Nb–5 mol%W alloy measured under the pressure condition of inlet/outlet = 0.05/0.01 MPa. In this case, as shown in Fig. 2, the hydrogen concentration at the inlet side is almost the same (i.e., about 0.2 (H/M)) for each system, but the difference of hydrogen chemical potential,  $\Delta\mu$ , is higher for ternary alloy than binary alloy. For example the values of  $\Delta\mu$  are about 4300 and 5200 J/mol for pressure conditions of inlet/outlet = 0.05/0.01 MPa and inlet/outlet = 0.1/0.01 MPa, respectively. In fact, the hydrogen flux is about 1.3 times higher for Nb–5 mol%W–5 mol%Mo alloy than Nb–5 mol%W alloy measured under these pressure conditions. In addition, the hydrogen flux for Nb–5 mol%W–5 mol%Mo alloy is more than 5 times higher than that for Pd–26 mol%Ag alloy. In this case, the  $c \times \Delta\mu$  value for Pd–26 mol%Ag alloy is very small compared to that for Nb-based alloys under these testing conditions.

A photo image of the sample disk for Nb–5 mol%W–5 mol%Mo alloy after hydrogen permeation test is shown in Fig. 5. There is no evidence of crack on the sample due to hydrogen embrittlement. Therefore, Nb–5 mol%W–5 mol%Mo alloy possesses excellent hydrogen permeability together with strong resistance to hydrogen embrittlement.

#### 4. Conclusion

The alloying effects of molybdenum on the hydrogen solubility, the resistance to hydrogen embrittlement and the hydrogen permeability of Nb–W alloy are investigated quantitatively. The hydrogen solubility decreases by the addition of molybdenum into Nb–W alloy or by increasing the temperature. As a result, the resistance to hydrogen embrittlement improves by reducing hydrogen concentration in the alloy. It is also found that Nb–5 mol%W–5 mol%Mo alloy possesses excellent hydrogen permeability without showing any hydrogen embrittlement when tested under appropriate permeation conditions.

#### Acknowledgements

This research was supported in part by the Japan Society for the Promotion of Science (JSPS) and by Research Foundation for Materials Science.

#### References

- [1] S.N. Paglieri, J.D. Way, Sep. Purif. Methods 31 (2002) 1–169.
- [2] K. Hashi, K. Ishikawa, T. Matsuda, K. Aoki, J. Alloys Compd. 368 (2004) 215–220.
- [3] C. Nishimura, M. Komaki, M. Amano, Mater. Trans. JIM 32 (1991) 501–507.
- [4] Y. Shinpo, H. Ohkouchi, M. Nishida, O. Kajita, S. Yamaura, H. Kimura, A. Inoue, Mater. Trans. 44 (2003) 1885–1890.
- [5] K. Komiya, Y. Shinzato, H. Yukawa, M. Morinaga, I. Yasuda, J. Alloys Compd. 404–406 (2005) 257–260.
- [6] S.A. Steward, Lawrence Livermore National Laboratory Reports, UCRL-53441, 1983.
- [7] Y. Matsumoto, H. Yukawa, T. Nambu, Metall. J. LXIII (2010) 74–78.
- [8] T. Nambu, K. Shimizu, Y. Matsumoto, R. Rong, N. Watanabe, H. Yukawa, M. Morinaga, I. Yasuda, J. Alloys Compd. 446–447 (2007) 588–592.
- [9] T. Nambu, Ph.D thesis, Nagoya University, Japan, 2006.
- [10] H. Yukawa, M. Morinaga, T. Nambu, Y. Matsumoto, Mater. Sci. Forum 654–656 (2010) 2827–2830.
- [11] H. Yukawa, T. Nambu, Y. Matsumoto, N. Watanabe, G.X. Zhang, M. Morinaga, Mater. Trans. 49 (2008) 2202–2207.
- [12] T.B. Massalski, J.L. Murray, L.H. Bennett, H. Baker, Binary Alloy Phase Diagrams, ASM, 1986.
- [13] T. Nambu, N. Shimizu, H. Ezaki, H. Yukawa, M. Morinaga, J. Jpn. Inst. Metals 69 (2005) 841–847.
- [14] E. Veleckis, R.K. Edwards, J. Phys. Chem. 73 (1969) 683–692.